



HAL
open science

Hexanuclear Molecular Precursors as Tools to Design Luminescent Coordination Polymers with Lanthanide Segregation

Haiyun Yao, Guillaume Calvez, Carole Daiguebonne, Yan Suffren, Kevin Bernot, Olivier Guillou

► **To cite this version:**

Haiyun Yao, Guillaume Calvez, Carole Daiguebonne, Yan Suffren, Kevin Bernot, et al.. Hexanuclear Molecular Precursors as Tools to Design Luminescent Coordination Polymers with Lanthanide Segregation. *Inorganic Chemistry*, 2021, 60 (21), pp.16782-16793. 10.1021/acs.inorgchem.1c02662 . hal-03414710

HAL Id: hal-03414710

<https://hal.science/hal-03414710v1>

Submitted on 10 Nov 2021

HAL is a multi-disciplinary open access archive for the deposit and dissemination of scientific research documents, whether they are published or not. The documents may come from teaching and research institutions in France or abroad, or from public or private research centers.

L'archive ouverte pluridisciplinaire **HAL**, est destinée au dépôt et à la diffusion de documents scientifiques de niveau recherche, publiés ou non, émanant des établissements d'enseignement et de recherche français ou étrangers, des laboratoires publics ou privés.



Distributed under a Creative Commons Attribution - NonCommercial 4.0 International License

Hexa-nuclear molecular precursors as tools to design luminescent coordination polymers with lanthanides segregation.

Haiyun Yao^{a,b}, Guillaume Calvez^{a,*}, Carole Daiguebonne^{a,*}, Yan Suffren^a, Kevin Bernot^a and Olivier Guillou^a

^a Univ Rennes, INSA Rennes, CNRS UMR 6226 "Institut des Sciences Chimiques de Rennes", F-35708 Rennes, France.

^b Present address: School of Opto-electronic Engineering, Zaozhuang University, Zaozhuang 277160, China.

* To whom correspondence should be addressed.

Guillaume.calvez@insa-rennes.fr

Carole.daiguebonne@insa-rennes.fr

ABSTRACT.

Solvothermal reactions between hexa-nuclear complexes with general chemical formula $[\text{Ln}_6(\mu_6\text{-O})(\mu_3\text{-OH})_8(\text{NO}_3)_6(\text{H}_2\text{O})_{12}]\cdot 2\text{NO}_3\cdot 2\text{H}_2\text{O}$ and 2-bromo-benzoic acid (2-bbH) lead to a series of isostructural one dimensional coordination polymers with general chemical formula $[\text{Ln}_2(2\text{-bb})_6]_\infty$ with Ln = Sm, Eu, Tb and Dy plus Y. These coordination polymers crystallize in the orthorhombic system, space group $Fdd2$ (n°43) with the following cell parameters: $a = 29.810(3) \text{ \AA}$, $b = 51.185(6) \text{ \AA}$, $c = 11.7913(14) \text{ \AA}$, $V = 17992(4) \text{ \AA}^3$ and $Z = 16$. The Eu- and Tb-based derivatives show sizeable luminescence intensities under UV excitation. Isostructural hetero-lanthanide coordination polymers have also been prepared. Their luminescent properties suggest that during the synthetic process the starting hexa-nuclear complexes are destroyed but strongly influence the distribution of the different lanthanide ions over the metallic sites of the crystal structure. Indeed, it is possible to prepare hetero-lanthanide coordination polymers in which the lanthanide ions segregation is controlled.

INTRODUCTION.

Lanthanide-based coordination polymers¹ attract great interest.²⁻⁷ Indeed, because of the unique optical⁸⁻⁹ and magnetic properties¹⁰ of the lanthanide ions, they present great interest in various technological fields such as molecular thermometry,¹¹⁻¹⁴ chemical sensing,¹⁵⁻¹⁷ light and display¹⁸⁻¹⁹ or fight against counterfeiting,²⁰⁻²³ for instance. Therefore, the quest for highly luminescent lanthanide-based coordination polymers is a continuous concern.^{13, 24-26} Because lanthanide ions present no structuring effect,²⁷ most of the reported studies focus their attention on the choice of the ligand.^{24-25, 28-33} This synthetic strategy offered very luminescent coordination polymers with high quantum yields.³⁴⁻³⁹ Some recent works suggest that an extended inorganic sub-lattice surrounded by ligands that act both as antennas and as spacers is relevant as far as highly luminescent coordination polymers are targeted.⁴⁰⁻⁴²

In order to obtain highly luminescent molecular materials a first approach is to optimize the ligand choice in order to gain on the relative organization of the metal centers as well as on the antenna effect toward them. In that way, our attention has been attracted by $[\text{Eu}(\text{2-bb})_3 \cdot \text{H}_2\text{O}]_\infty$ that is, to the best of our knowledge, the only reported lanthanide-based coordination polymer with 2-bromobenzoate ligand (hereafter symbolized by 2-bb⁻). This compound, described by Wu *et al.* in 2009⁴³ crystallizes in the monoclinic system, space group $P2_1/n$ (n°14) with the following cell parameters: $a = 12.530(3) \text{ \AA}$, $b = 6.9534(14) \text{ \AA}$, $c = 26.079(5) \text{ \AA}$, $\beta = 101.65(3)^\circ$, $V = 2225.5(8) \text{ \AA}^3$ and $Z = 4$ (CCDC-672310). It has been obtained by solvothermal synthesis. The crystal structure can be described on the basis of 1D molecular chains (Figure 1). This crystal structure presents a 1D inorganic sub-lattice (coordination polyhedrons share edges) decorated by 2-bb⁻ ligands that act both as spacers and as antennas. Indeed, this ligand presents an extended conjugated π system that can provide both an efficient antenna effect⁴⁴ and π -stacking interactions. Actually, the authors indicated that this compound exhibits an intense luminescence.

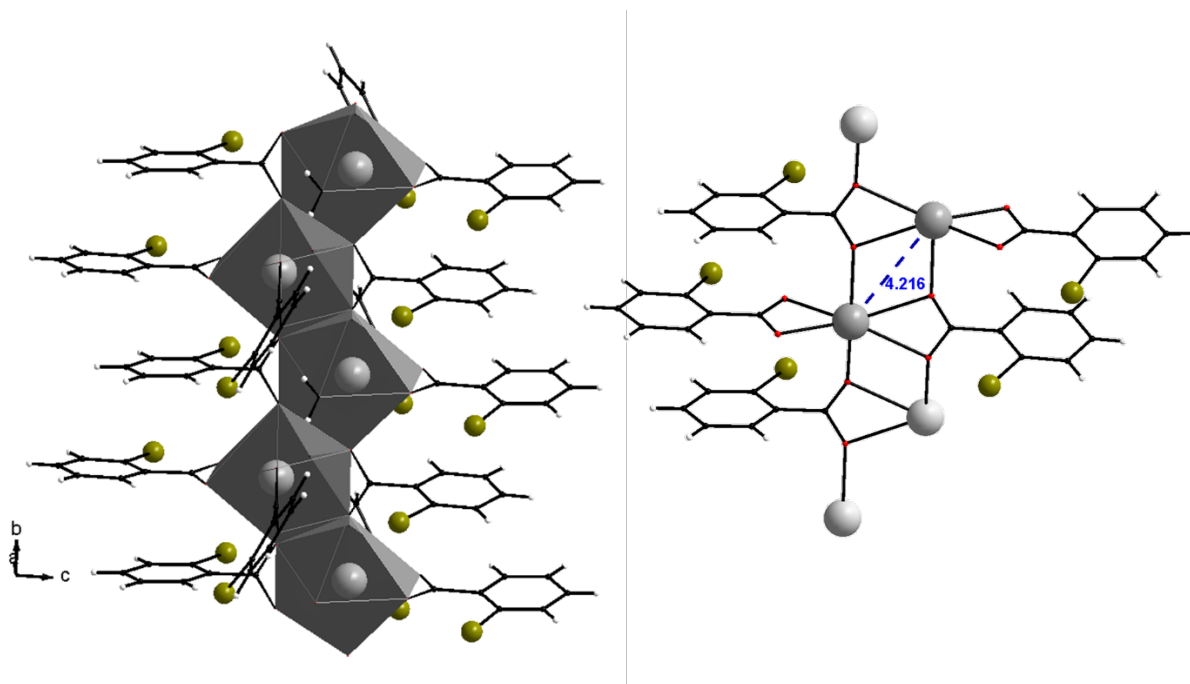


Figure 1. Projection view of the 1D molecular chain (left) and schematic representation of the inorganic sub-lattice (right) of $[\text{Eu}(2\text{-bb})_3\cdot\text{H}_2\text{O}]_\infty$. Only the binding ligands have been drawn. Redrawn from reference 43. The shortest intermetallic distance is reported in Å.

Another approach focuses on the optimization of the metal center toward optical emission. Indeed, it has been shown that it is possible to build lanthanide-based coordination polymers in which the metallic centers are no longer single lanthanide ions but poly-lanthanide complexes.⁴⁵⁻⁴⁷ However, although many beautiful compounds based on such entities have been reported to date,⁴⁸⁻⁵¹ most of them have been obtained by serendipitous one-pot syntheses.^{22, 52} Rational design of such coordination polymers requires stable poly-lanthanide oxo/hydroxo complexes that can be used as starting materials. However, up-to-date, the only poly-lanthanide complexes stable enough to act as molecular precursors are the hexa-nuclear complexes with a $[\text{Ln}_6(\mu_6\text{-O})(\mu_3\text{-OH})_8]^{8+}$ core, first described by Zack *et al.* (Figure 2).⁵³⁻⁵⁷

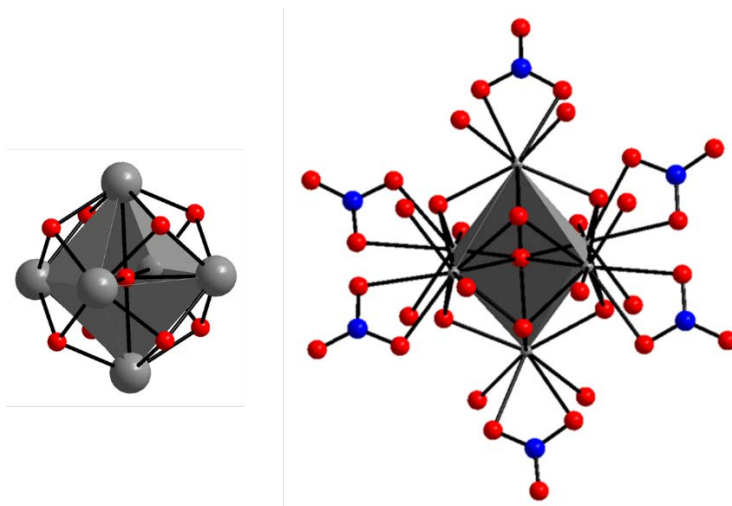


Figure 2. Octahedral hexa-nuclear core $[\text{Ln}_6(\mu_6\text{-O})(\mu_3\text{-OH})_8]^{8+}$ (left) and projection view of $[\text{Y}_6(\mu_6\text{-O})(\mu_3\text{-OH})_8(\text{NO}_3)_6(\text{H}_2\text{O})_{12}]^{2+}$ (right). Hydrogen atoms have been omitted for clarity. Redrawn from reference 57.

When these octahedral complexes are used as molecular precursors they can lead to coordination polymers,⁴⁵ complexes⁵⁸⁻⁵⁹ or colloidal suspensions.⁶⁰ During the synthetic process, the octahedral arrangement is more or less modified,^{45, 58-59} depending on the synthesis. However, even when the hexa-nuclear core is destroyed, hexa-nuclear complexes used as reactants present a structuring effect and lead to original crystal structures that cannot be obtained using mono-nuclear lanthanide salts.⁶¹⁻⁶² It can be noticed that, in this octahedral core, lanthanide ions are about 3.5 Å far from each other, which is close to the distance between two lanthanide ions bridged by a carboxylate group.


In this manuscript, we combine the two strategies described above by using an efficient ligand for the organization of metallic centers and their sensitization via antenna effect, with the use of original hexa-nuclear cores as metallic centers. We thus describe the synthesis, the crystal structure and the luminescence properties of 1D coordination polymers obtained by reaction between 2-bromo-carboxylic acid and, no longer single lanthanide ions, but hexa-nuclear complexes.

EXPERIMENTAL SECTION.

Synthesis of $[\text{Ln}_2(2\text{-bb})_6]_\infty$ with Ln = Sm, Eu, Tb, Dy plus Y.

Lanthanide oxides (4N) were purchased from Ampere and used without further purification. Lanthanide nitrates were prepared according to established procedures.⁶³ Hexa-nuclear complexes with general chemical formula $[\text{Ln}_6(\mu_6\text{-O})(\mu_3\text{-OH})_8(\text{NO}_3)_6(\text{H}_2\text{O})_{12}] \cdot 2\text{NO}_3 \cdot 2\text{H}_2\text{O}$ with Ln = Sm, Eu, Tb and Dy plus Y (hereafter symbolized by $[\text{Ln}_6]$) (Figure 2) were prepared as previously described.^{57, 64} Hetero-lanthanide hexa-nuclear complexes were synthesized according to previously published procedures.⁶⁵ 2-bromo-benzoic acid was purchased from TCI (>98%) and used without further purification.

0.005 mmol of a hexa-nuclear complex ($[\text{Ln}_6]$), 0.05 mmol of 2-bromo-benzoic acid (2-bbH) and 2 mL of acetonitrile were placed in a 24 mL Parr autoclave. The molar ratio hexa-nuclear complex / ligand (1 / 10) has been used to fit with the number of basic oxo/hydroxo groups per hexa-nuclear complex.⁵² The Parr autoclaves were heated at 100-120°C (depending on the lanthanide ion) for 100 h (Table 1). Then the autoclaves were cooled down at a 2°C.h⁻¹ cooling rate. Colorless single crystals were obtained that were filtered, washed with acetonitrile and dried in ambient conditions.

Table 1. Details of the syntheses of $[\text{Ln}_2(2\text{-bb})_6]_\infty$ with Ln = Sm, Eu, Tb, Dy, Y		
Ln ³⁺	Temperature (°C)	Pictures of single crystals under UV excitation (312 nm)
Sm ³⁺	110	
Eu ³⁺	110	
Tb ³⁺	115	
Dy ³⁺	115	
Y ³⁺	120	

It must be noticed that each batch produces only about 150 µg of crystals, which prevents us from performing measurements that require big amounts of powder (all measurements have been done on the basis of crushed single crystals). Isostructurality of the

compounds was assumed on the basis of their powder X-ray diffraction diagrams and of their IR spectra. All of them were similar and only those of the Dy-derivative are reported, as a matter of example (Figures S1 and S2).

X-ray diffraction.

Powder X-ray diffraction diagrams were collected with a Panalytical X'Pert Pro diffractometer equipped with an X'Celerator detector. Typical recording conditions were: 45 kV, 40 mA, Cu K_{α} radiation ($\lambda = 1.542 \text{ \AA}$), θ/θ mode. Simulated patterns from crystal structure were produced with PowderCell and WinPLOTR programs.⁶⁶⁻⁶⁸

The crystal structure has been solved on the basis of the dysprosium derivative. Single crystals were mounted on a Bruker D8 Venture diffractometer. Crystal data collection were performed at 150 K with Mo K_{α} radiation ($\lambda = 0.70713 \text{ \AA}$). The crystal structure was solved, using SIR 97,⁶⁹ by direct methods. It was refined, using SHELX-2017⁷⁰⁻⁷¹ with the aid of WINGX program.⁷²⁻⁷³ Most of non-hydrogen atoms were refined anisotropically. Because of the quite large unit cell ($V = 17992 \text{ \AA}^3$) some of them have been refined isotropically for a better convergence of the refinement. Hydrogen atoms were located at ideal positions. Absorption corrections were performed using the facilities of WINGX program.⁷⁴ Selected crystal and final structure refinement data are gathered in Table 2. Full details of the crystal structure have been deposited with the Cambridge Crystallographic Data Center under the depository number CCDC-1871220.

Chemical formula	$\text{C}_{42}\text{H}_{24}\text{Br}_6\text{Dy}_2\text{O}_{12}$
System	Orthorhombic
Space group (n°)	$Fdd2$ (n°43)
Formula weight (g.mol^{-1})	1525.01
a (Å)	29.810(3)
b (Å)	51.185(6)
c (Å)	11.7913(14)
V (Å ³)	17992(4)
Z	16
D_{calc} (g.cm^{-3})	2.252
R (%)	4.48
R_w (%)	10.85
GoF	1.044
CCDC number	1871220

Electronic microscopy and Energy Dispersive Spectroscopy (EDS).

EDS measurements have been performed with a Hitachi TM-1000, Tabletop Microscope version 02.11 (Hitachi High-Technologies, Corporation Tokyo Japan) with EDS analysis system (SwiftED-TM, Oxford Instruments Link INCA). Reproducibility of the elemental analyses has been checked by repeating the measurements several times. Results, expressed in atom percentages, are average values of different spots. These experiments support the homogeneity of the samples.

Optical measurements.

Solid-state emission and excitation spectra have been measured on a Horiba Jobin-Yvon Fluorolog III fluorescence spectrometer equipped with a Xe lamp 450 W, an UV-Vis photomultiplier (Hamamatsu R928, sensitivity 190 - 860 nm). The emission/excitation spectra recordings were realized on powder samples in 700 μL quartz cuvettes. The low temperature fluorescence measurement on Y-based sample was realized with the same device in a quartz capillary using a Dewar filled with liquid nitrogen, at 77 K. The quantum yields were measured with the same device using an integrating sphere, extending its correction curve in the 290-330 nm range by measuring standards in this range (the Eu tris-dipicolinate in *tris*

(tris(hydroxymethyl)aminomethane) buffer solution as proposed by Chauvin *et al.*⁷⁵). The quantum yield was estimated measuring the ratio between absorbed photons around the excitation wavelength without and with the sample (the difference between respectively L_a and L_c values for corresponding integrated spectra) and the emitted photons with and without the sample (the difference between respectively E_c and E_a values for corresponding integrated spectra). The lifetime values were measured with the same device, using a pulsed Xenon source and measuring the intensity emitted after increasing time delay. The decay time was then fitted using a mono-exponential decay function. Appropriate filters were used to remove the residual excitation laser light, the Rayleigh scattered light and associated harmonics from spectra. All spectra were corrected for the instrumental response function. The absorbance spectrum at room temperature was realized using a Perkin Elmer Lambda 650 dual beam spectrometer with an integrating sphere allowing the measurement of solid-state samples. Colorimetric coordinates have been calculated on the basis of the emission spectra.⁷⁶⁻⁷⁷ IR spectra were recorded between 4000 and 400 cm^{-1} using a Perkin Elmer Frontier FTIR spectrometer equipped with an ATR sampling accessory.

RESULTS AND DISCUSSION.

Reactions in solvothermal conditions between an hexa-nuclear complex ($[\text{Ln}_6(\mu_6\text{-O})(\mu_3\text{-OH})_8(\text{NO}_3)_6(\text{H}_2\text{O})_{12}] \cdot 2\text{NO}_3 \cdot 2\text{H}_2\text{O}$) and 2-bromo-benzoic acid (2-bbH) in acetonitrile lead to lanthanide-based one-dimensional coordination polymers with general chemical formula $[\text{Ln}_2(2\text{-bb})_6]_\infty$ with Ln = Sm, Eu, Tb and Dy plus Y.

Crystal structure description.

The crystal structure was solved on the basis of the Dy-derivative. It crystallizes in the orthorhombic system, space group $Fdd2$ ($n^\circ 43$) (See Table 1).

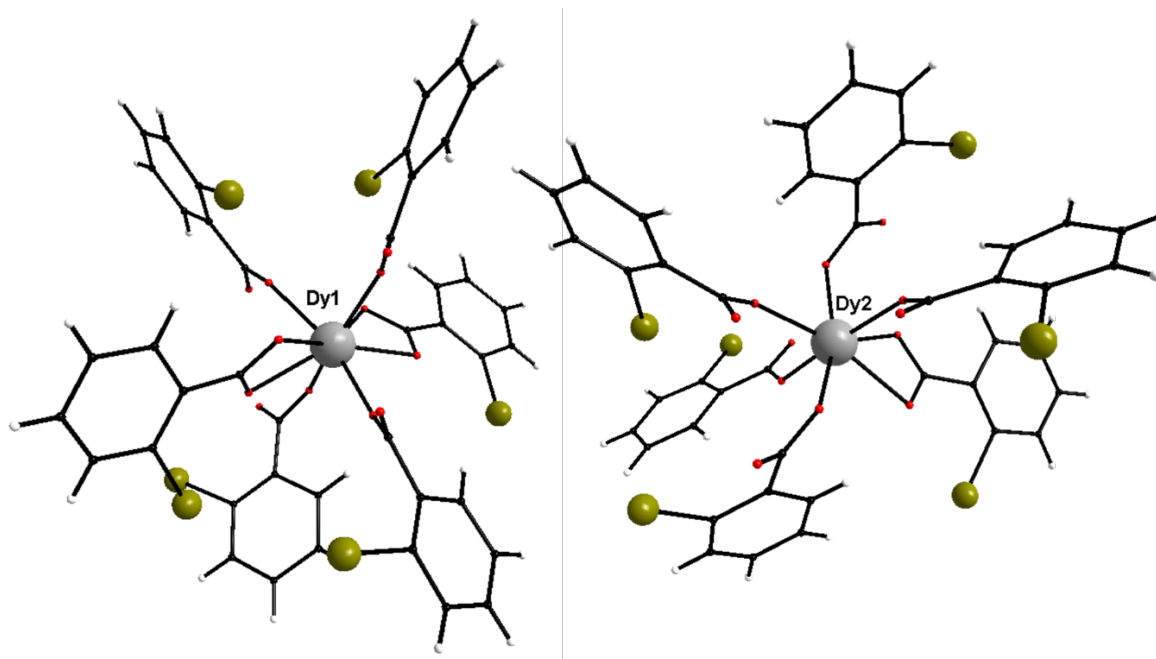


Figure 3. Perspective views of the neighborhoods of the two independent Dy^{3+} ions in $[\text{Dy}_2(2\text{-bb})_6]_\infty$.

There are two independent Dy^{3+} ions and six independent 2-bb⁻ ligands in the asymmetric unit. Dy1 is eight coordinated by eight oxygen atoms from six different 2-bb⁻ ligands that form a slightly distorted snub diphenoid (Continuous Shape Measurements(CShM)⁷⁸⁻⁷⁹ agreement factor is 2.958 - See Table S1). Dy2 is seven coordinated by seven oxygen atoms from six different 2-bb⁻ ligands that form a slightly distorted pentagonal bi-pyramid (Continuous Shape Measurements(CShM) agreement factor is 1.119 – See Table S1) (Figure 3). The ligands present two μ_2 binding modes. The first one binds the two Dy^{3+} ions in a monodentate way while the second one binds one Dy^{3+} ion in a monodentate way and the other in a bidentate way (Figure 4). It can be noticed that in this crystal structure there is no coordination or crystallization solvent molecule. The ligands triply bridge the Dy^{3+} ions, which leads to 1D molecular chains in which the Dy^{3+} coordination polyhedrons alternatively share an edge or a vertex forming a 1D inorganic sub-lattice (Figure 4). Intermetallic distances between neighboring Dy^{3+} ions in the molecular chain are 3.8771(9) Å and 4.2296(9) Å.

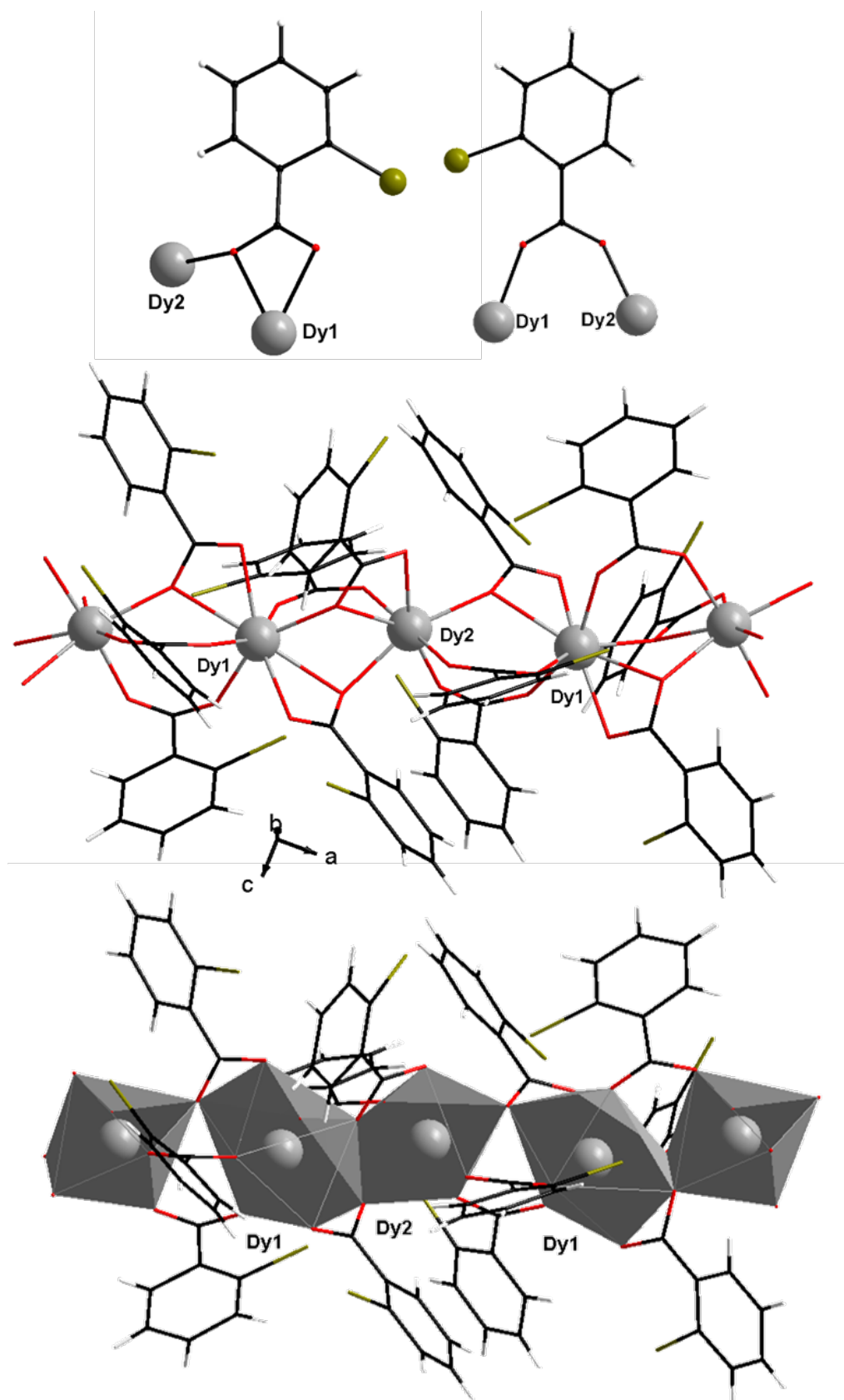
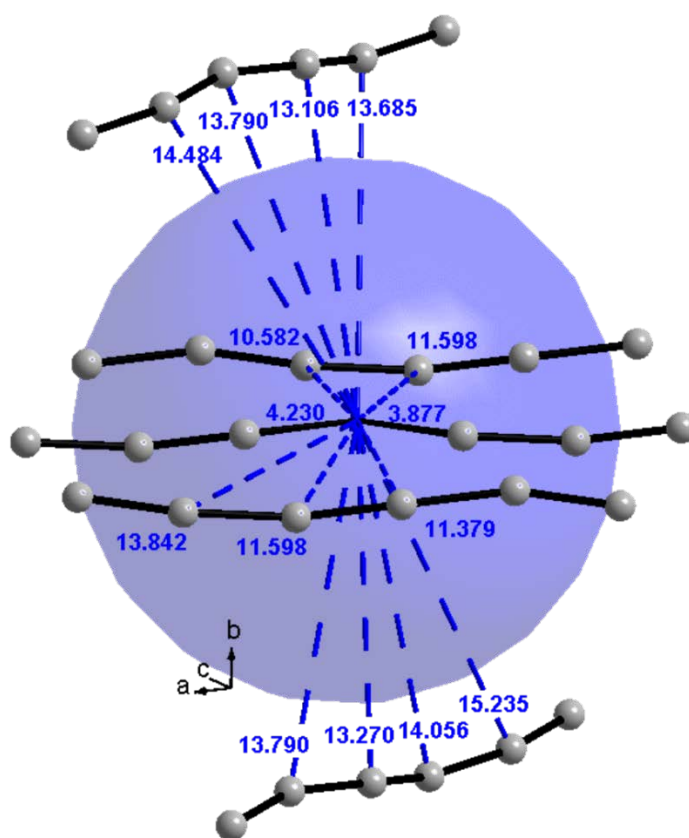


Figure 4. Ligands binding modes in $[\text{Dy}_2(2\text{-bb})_6]_\infty$ (top). Projections views of a molecular chain in $[\text{Dy}_2(2\text{-bb})_6]_\infty$ (middle). Projections views of a molecular chain in $[\text{Dy}_2(2\text{-bb})_6]_\infty$ with Dy^{3+} coordination polyhedrons (bottom).

There are 2- bb^- ligands all around these inorganic chains that therefore are quite far away from each other (Scheme 1). Indeed, the shortest distances between Dy^{3+} ions that belong to adjacent chains are greater than 10 Å, that is the distance above which intermetallic energy transfers⁸⁰⁻⁸¹ are expected to be less efficient.⁸²⁻⁸³ The only intermetallic distances shorter than this threshold are those between lanthanide ions that belong to the same molecular chains. Consequently, there are only four Dy^{3+} ions closer than 10 Å from a given Dy^{3+} ion (Scheme 1). Projection views of a unit cell content are reported in Figure 5



Scheme 1. Schematic representation of $[Dy_2(2-bb)_6]_\infty$. Only lanthanide ions are drawn for clarity. Shortest intermetallic distances from a given atom (Dy1 in blue) are reported (in Å). The diameter of the blue sphere is 10 Å.

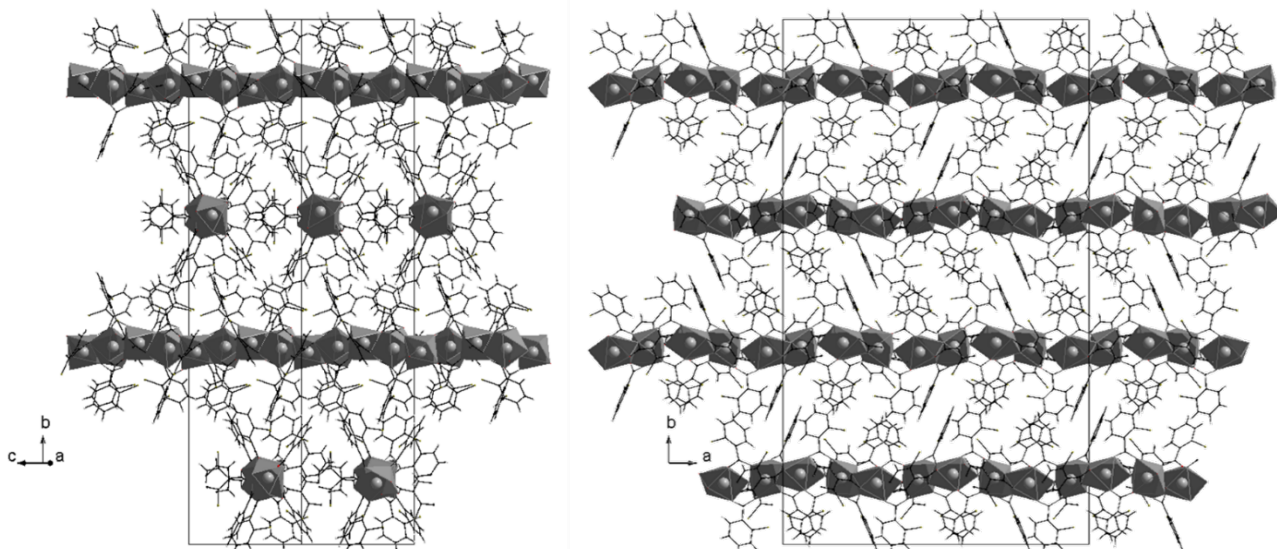


Figure 5. Projection views of an extended unit cell of $[\text{Dy}_2(2\text{-bb})_6]_\infty$ along the $a+c$ direction (left) and along the c -axis (right). Coordination polyhedrons have been drawn.

Luminescent properties of $[\text{Ln}_2(2\text{-bb})_6]_\infty$ with $\text{Ln} = \text{Tb}$ and Eu .

Room temperature solid-state excitation and emission spectra of the Tb^{3+} - and Eu^{3+} -derivatives have been recorded (Figure 6). In both excitation spectra there is a broad excitation band centered at 300 nm that can be attributed to the ligand ${}^1\pi^*/{}^3\pi^* \leftarrow {}^1\pi$ transitions. Energies of the first excited singlet (${}^1\pi^*$) and triplet (${}^3\pi^*$) states of the ligand have been estimated by referring to the UV-visible absorbance edge (320 nm \approx 31250 cm^{-1}) (Figure S3) and to the phosphorescent band recorded at 77 K (423 nm \approx 23640 cm^{-1}) (Figure S4) of the Y-derivative. According to Reinhoudt's empirical rules,⁸⁴ the gap between the first excited triplet state and single state (7600 cm^{-1} > 5000 cm^{-1}) is expected to favor efficient Inter-System-Crossing. On another hand, according to Latva's empirical rules,⁸⁵ the energy of the first excited triplet state of the ligand is expected to favor good ligand-to-lanthanide energy transfers for both the terbium and the europium ions. This suggests the presence of an efficient antenna effect.⁴⁴ The efficiency of this effect has been estimated using the following relationship on the basis of the Eu-derivative:⁸³

$$Q_{Ln}^{Ligand} = \eta_{sens} \cdot Q_{Ln}^{Ln} \quad (1.)$$

where Q_{Ln}^{Ligand} and Q_{Ln}^{Ln} are the overall and intrinsic quantum yields, respectively, and where η_{sens} is the sensitization efficiency (via antenna effect) (Table 3). The intrinsic quantum yield has been recorded at 395 nm which is a 4f-4f transition ($Eu^{3+}: ^5L_6 \leftarrow ^7F_0$)⁸⁶ without significant overlap with the ligand absorption band. The sizeable value⁸⁷ of the sensitization efficiency, 69(6) %, confirms the efficiency of the antenna effect and is in agreement with the overall quantum yields that have been measured. It can also be noticed that both the Eu- and the Tb-derivatives present similar quantum yields. This may be related to the absence of C-H and O-H vibrators near the lanthanide ions.

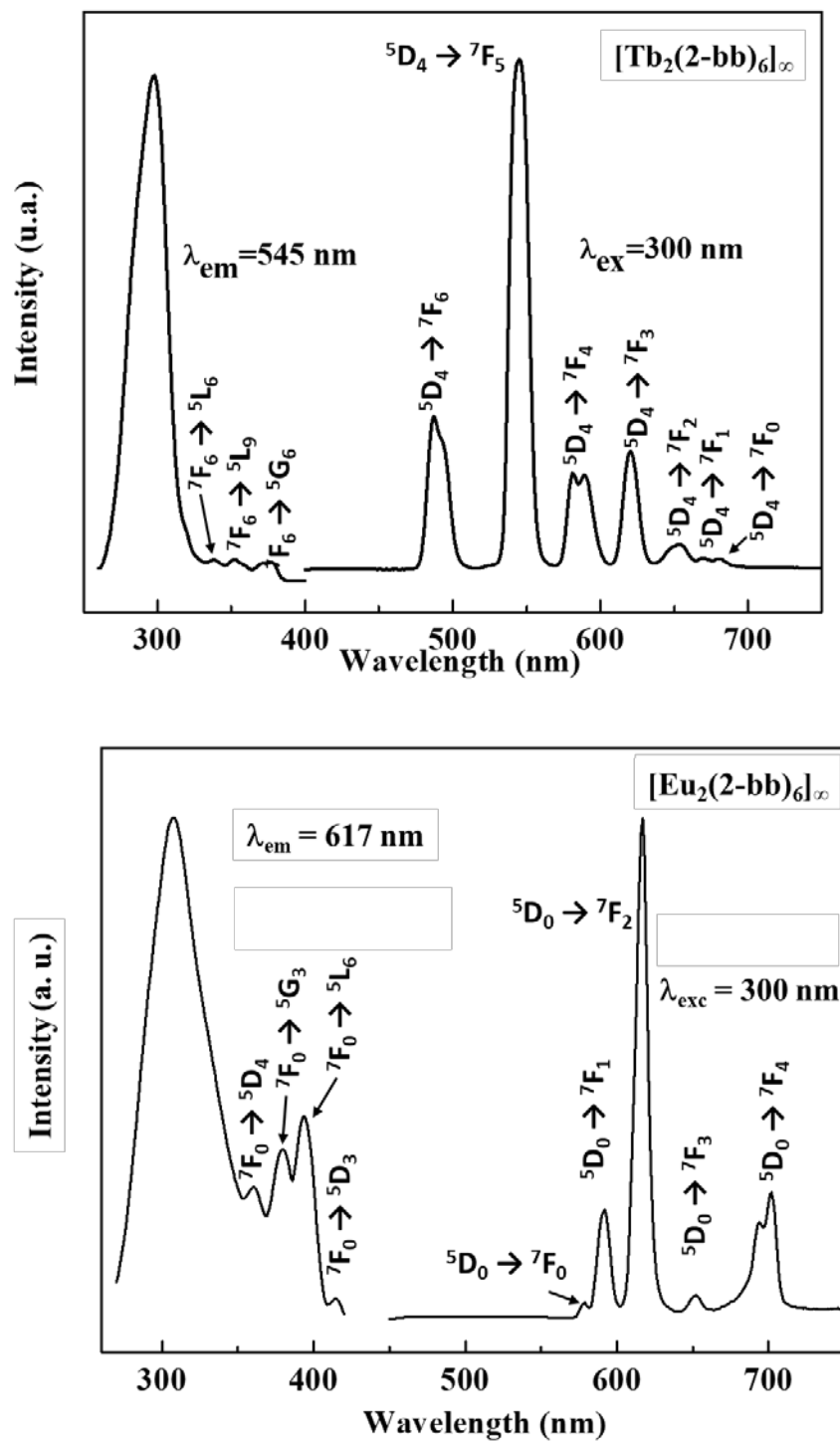


Figure 6. Solid-state room temperature excitation and emission spectra of [Tb₂(2-bb)₆]_∞ (top) and of [Eu₂(2-bb)₆]_∞ (bottom). λ_{exc} = 300 nm.

Table 3. Colorimetric coordinates, quantum yields and luminescent lifetimes for $[\text{Tb}_2(2\text{-bb})_6]_\infty$ and $[\text{Eu}_2(2\text{-bb})_6]_\infty$.

	$Q_{\text{Ln}}^{\text{Ligand}}$ (%)	τ (ms)	$Q_{\text{Ln}}^{\text{Ln}}$ (%)	η_{sens} (%)	Colorimetric coordinates	
					x	y
$[\text{Tb}_2(2\text{-bb})_6]_\infty$	16(1)	0.97(5)	-	-	0.349	0.597
$[\text{Eu}_2(2\text{-bb})_6]_\infty$	11(1)	0.48(4)	16(1)	69(6)	0.629	0.345

Concentration quenching: Luminescence properties of $[\text{Y}_{2x}\text{Tb}_{2-2x}(2\text{-bb})_6]_\infty$ with $0.05 \leq x \leq 0.9$.

The quite moderate quantum yield of the Tb^{3+} -derivative suggests a strong concentration quenching effect related to intermetallic energy transfers. In order to verify this assumption some hetero-lanthanide compounds with general chemical formula $[\text{Y}_{2x}\text{Tb}_{2-2x}(2\text{-bb})_6]_\infty$ have been prepared from the corresponding $[\text{Y}_{6x}\text{Tb}_{6-6x}]$ hetero-lanthanide molecular precursors.⁶⁰ In these compounds dilution of the optically active Tb^{3+} ions by optically non-active Y^{3+} ions, that statistically increases the mean Tb-Tb distance, is expected to produce an enhancement of the luminescence of the Tb^{3+} ions.⁸⁷ Their overall quantum yields and luminescent lifetimes have been measured ($\lambda_{\text{exc}} = 300$ nm) (Table 4 and Figure 7). Emission spectra are reported in Figure S5.

Table 4. Relative ratios between Y^{3+} and Tb^{3+} , Tb^{3+} overall quantum yields and luminescent lifetimes for some $[\text{Y}_{2x}\text{Tb}_{2-2x}(2\text{-bb})_6]_\infty$ compounds with $0 < x < 1$.

x^b	Tb^a (%)	Y^a (%)	$Q_{\text{Ln}}^{\text{Ligand}}$ (%)	τ (ms)
0.05	96(2)	4(2)	24(2)	1.0(1)
0.1	88(2)	12(2)	36(3)	1.2(1)
0.25	75(2)	25(2)	14(1)	0.9(1)
0.5	54(2)	46(2)	10(1)	1.1(1)
0.66	34(2)	66(2)	9(1)	0.9(1)
0.9	13(2)	87(2)	9(1)	0.9(1)

a: Experimental values (metal contents found by elemental analyses)

b: Expected values

At this point, one must notice that the x values is an average value that correspond to a mixture of several complexes with different distributions of the two lanthanide ions over the metallic sites of the complexes.⁶⁵ Because they are hexa-lanthanide complexes, x value for a

given complex can only be 0, 1/6, 2/6, 3/6, 4/6, 5/6 and 1. Additionally, because ionic radii of the Tb^{3+} and Y^{3+} ions are quite different, *trans* configurations are probably favored with respect with *cis* configurations (which is also in agreement with the inversion center on the central oxygen atom).

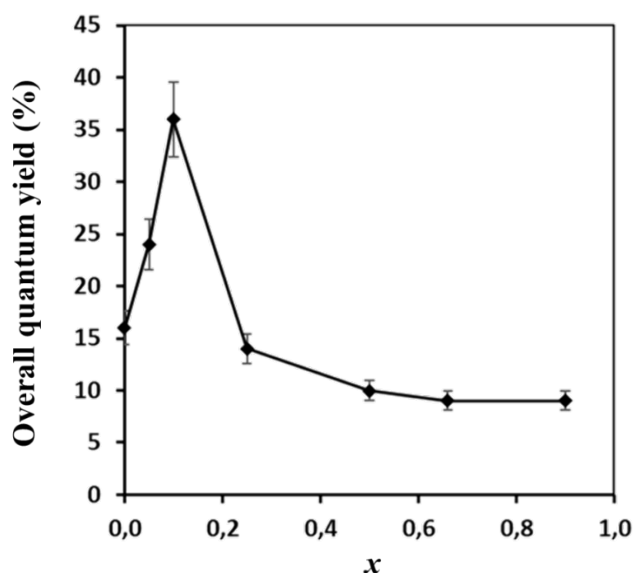


Figure 7. Tb^{3+} overall quantum yields for some $[\text{Y}_{2x}\text{Tb}_{2-2x}(\text{2-bb})_6]_{\infty}$ compounds with $0 \leq x < 1$ ($\lambda_{\text{exc}} = 300 \text{ nm}$).

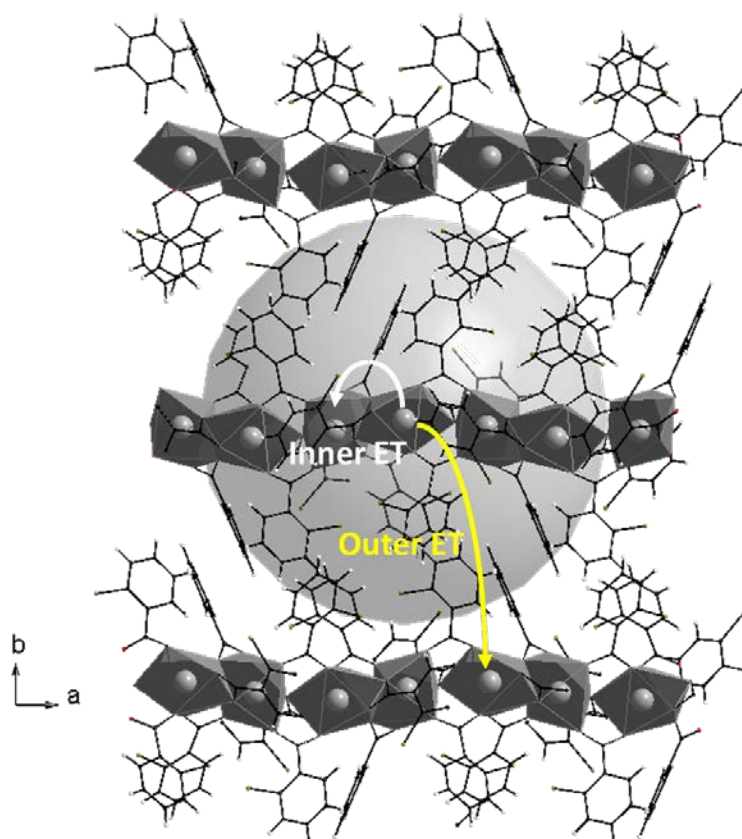
These measurements strongly suggest that the distribution of the lanthanide ions over the metallic sites of the molecular chain crystal structure is influenced by the composition of the hexa-nuclear molecular precursor. Indeed, if the hexa-nuclear complexes were completely destroyed before the building of the molecular chains, the distribution of the lanthanide ions would be perfectly random⁸⁷ and the overall quantum yield *versus* x curve would be similar to those that are commonly observed for actual molecular alloys prepared from simple lanthanide salts (such as chlorides or nitrates) in water.⁸⁸

If it was the case one would expect to observe a maximum of the quantum yield when statistically there are only non-optically active lanthanide ions in a 10 \AA radius sphere centered on a given optically active lanthanide ion, that is, in the present case, for $x \approx 80\%$ (Since there are four lanthanide ions closer than 10 \AA from a given lanthanide ion. See Scheme 2). On the

contrary, the observed quantum yield abruptly increases by about 50% as soon as only 5% of Y^{3+} are present. This suggests that there are some part of the molecular chains in which Tb^{3+} ion are further from each other than the mean Tb-Tb distance. These parts contribute to an enhancement of the overall luminescence of the crystal.

These measurements also show that after a strong dilution effect, that can be attributed to an increase of the Tb-Tb distance in a molecular chain, the dilution effect is then less efficient and simply compensates the decrease of the number of the emitting lanthanide ions. This is in agreement with the big intermetallic distances between lanthanide ions that belong to neighboring molecular chains.

Indeed, based on the crystal structure analysis, one can expect two different modes of intermetallic energy transfers: a very efficient one inside the chains (inner intermetallic energy transfer) and a less efficient one between lanthanide ions that belong to neighboring molecular chains (outer energy transfer) (Scheme 2).



Scheme 2. Schematic representation of the inner and outer energy transfers. The 10 Å radius sphere symbolizes the zone in which intermetallic energy transfers are expected to be the more efficient.

Intermetallic energy transfers have been studied extensively.⁸⁹⁻⁹⁰ Two mechanisms originate them: The first one, which is encountered in molecular species, is due to electrostatic interactions and is independent from the concentration of both the donor and the acceptor. It relies only with a well-defined donor/acceptor pair.^{81, 91} The second one, which is encountered in doped infinite materials, is related to exchange interactions and depends on the statistical distribution of the donors and acceptors.^{80, 92} Therefore, it must vary with the doping rate.

Energy transfer efficiency: Luminescence properties of $[\text{Eu}_{2x}\text{Tb}_{2-2x}(\text{2-bb})_6]_{\infty}$ with $0.05 \leq x \leq 0.5$.

The strong dilution effect highlighted above suggests efficient intermetallic energy transfers. Therefore some hetero-lanthanide compounds with general chemical formula $[\text{Eu}_{2x}\text{Tb}_{2-2x}(\text{2-bb})_6]_{\infty}$ have been prepared from the corresponding $[\text{Eu}_{6x}\text{Tb}_{6-6x}]$ hetero-lanthanide hexa-nuclear precursors (Table 5). The study was limited to x smaller than 0.5 because when x becomes greater than 0.5, the luminescence of the Tb^{3+} ion almost vanishes. Emission spectra have been recorded (Figure 8) and luminescence lifetimes and overall quantum yields have been measured under UV irradiation ($\lambda_{\text{exc}} = 300 \text{ nm}$) (Table 5). Intermetallic energy efficiency (η_{ET}) of these compounds have also been calculated according to the relationship:⁸³

$$\eta_{\text{ET}} = 1 - \frac{\tau_{\text{obs}}}{\tau_0} \quad (2.)$$

where τ_0 (Table 4) and τ_{obs} (Table 5) are the Tb^{3+} luminescence lifetimes in the absence and in the presence of Eu^{3+} acceptor ions, respectively.

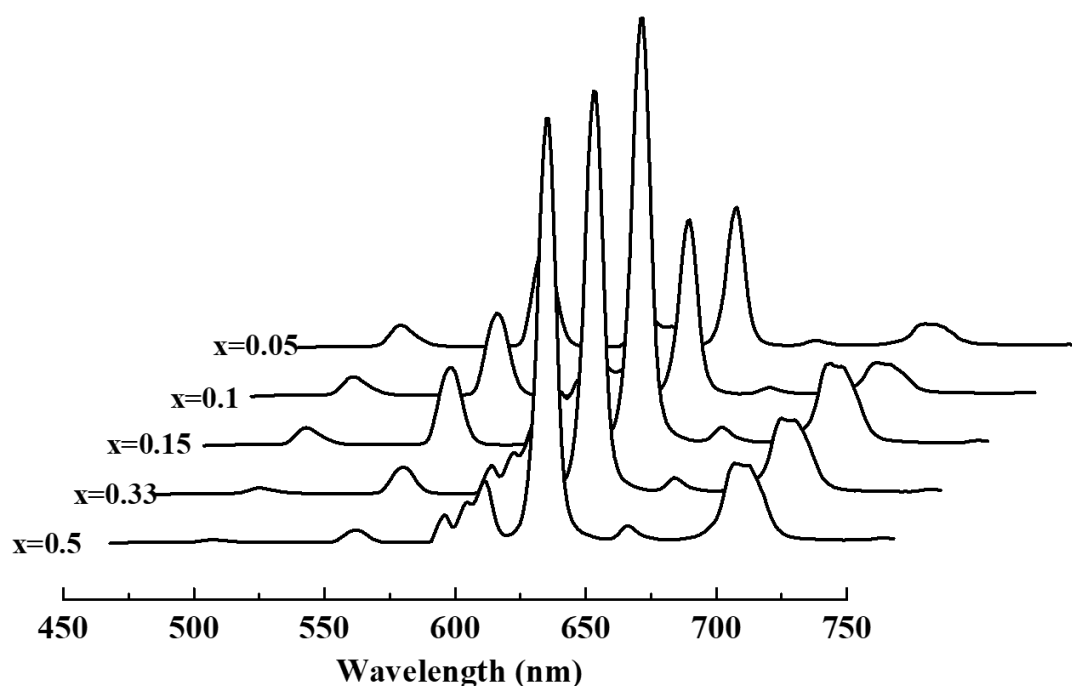


Figure 8. Room temperature solid-state emission spectra of $[\text{Eu}_{2x}\text{Tb}_{2-2x}(\text{2-bb})_6]_{\infty}$ with $0.05 \leq x \leq 0.5$ under UV irradiation ($\lambda_{\text{exc}} = 300 \text{ nm}$).

Table 5. Relative contents, overall quantum yields and luminescence lifetimes of Eu^{3+} and Tb^{3+} and intermetallic energy transfer efficiency for $[\text{Eu}_{2x}\text{Tb}_{2-2x}(\text{2-bb})_6]_{\infty}$ with $0.05 \leq x \leq 0.5$.

x^b	$\text{Eu}^a(\%)$	$\text{Tb}^a(\%)$	$Q_{\text{Eu}}^{\text{Ligand}} \%$	$\tau \text{ (ms)}$	$Q_{\text{Tb}}^{\text{Ligand}} \%$	$\tau \text{ (ms)}$	$\eta_{\text{ET}} (\%)$
0.05	9(2)	91(2)	4.3(4)	0.75(7)	3.1(3)	0.37(4)	63(6)
0.1	12(2)	88(2)	8.6(8)	0.70(7)	3.6(4)	0.24(2)	76(7)
0.2	20(2)	80(2)	7.4(7)	0.68(7)	1.1(1)	0.14(1)	85(8)
0.33	34(2)	66(2)	6.9(7)	0.60(6)	0.64(6)	0.08(1)	92(9)
0.5	49(2)	51(2)	8.2(8)	0.60(6)	0.44(4)	0.05(1)	95(9)

a: Experimental values (metal contents found by elemental analyses)

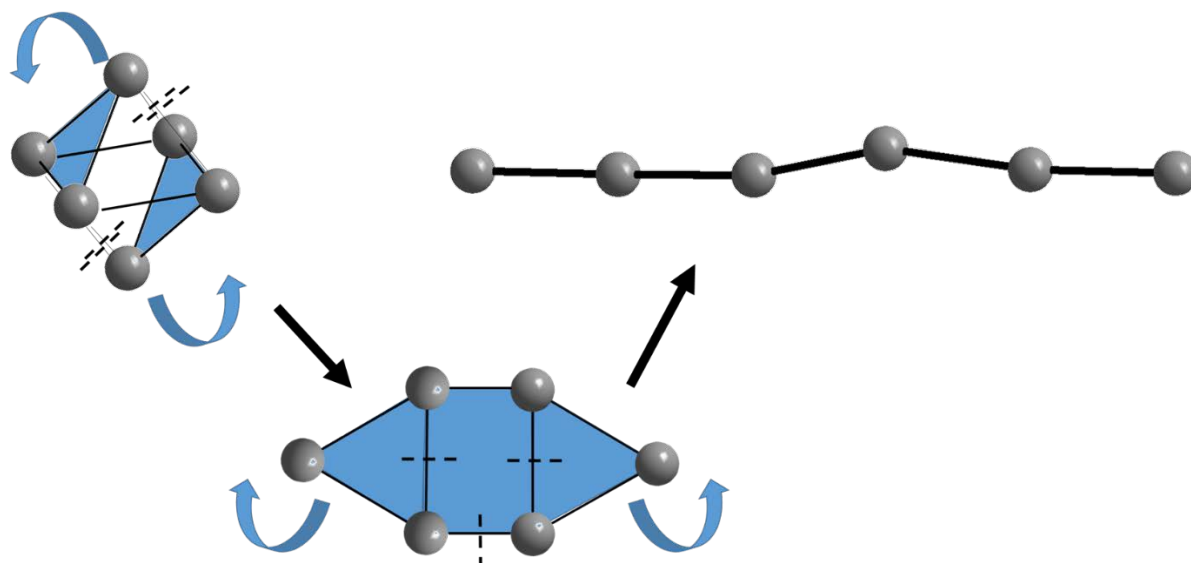
b: Expected values (metal contents used for the synthesis)

These measurements confirm that there is strong, and rapidly growing with x , intermetallic energy transfers in this series of compounds. This is in agreement with the short intermetallic distances in the molecular chains. This also strongly suggests that intermetallic energy transfers, in this series of compounds, are due to exchange interactions.

Suggested synthetic mechanism.

In order to check if the hexa-nuclear complexes actually play a role in the synthetic process, reaction between lanthanide nitrates (that can be considered in wet acetonitrile as a mono-lanthanide complexes)⁹³ and 2-bromo-benzoic acid were realized in identical conditions. In any cases, no crystallization or precipitation occurred.

It has been previously shown for a similar system⁵⁸ that the carboxylate oxygen atoms binding and the collapse of the starting hexa-nuclear complex occur simultaneously. Indeed, the carboxylate functions clip and connect neighboring lanthanide ions while the capping hydroxyl groups are removed. The proposed mechanism was the separation and the gliding of two opposite triangular faces of the starting octahedron forming a hexagonal ring (Scheme 3). In the present case, based on this mechanism, it can be suggested that the transformation goes on and finally leads to a straight molecular chain.



Scheme 3. Suggested synthetic mechanism: separation and gliding of the two opposite triangular faces, separation of the two triangles and resulting chain. Broken lines symbolize bond breaking.

Comparison between the luminescence properties of $[\text{EuTb}(\text{2-bb})_6]_\infty$ and $\{[\text{Tb}_2(\text{2-bb})_6]_{0.5}[\text{Eu}_2(\text{2-bb})_6]_{0.5}\}_\infty$.

If this suggested mechanism really occurs, hetero-lanthanide molecular chains must be different depending on whether the starting octahedral complexes are homo- or hetero-lanthanide.

In order to verify this assumption, two compounds, with identical elemental composition and overall crystal structure, have been prepared in identical synthetic conditions: (i) $[\text{EuTb}(\text{2-bb})_6]_\infty$ has been prepared from the single $[\text{Eu}_3\text{Tb}_3]$ hexa-nuclear precursor; (ii) $\{[\text{Tb}_2(\text{2-bb})_6]_{0.5}[\text{Eu}_2(\text{2-bb})_6]_{0.5}\}_\infty$ has been prepared from a fifty-fifty mixture of $[\text{Eu}_6]$ and $[\text{Tb}_6]$ hexa-nuclear precursors (Scheme 4).

Their emission spectra have been recorded ($\lambda_{\text{exc}} = 300 \text{ nm}$) (Figure 9) and their colorimetric coordinates calculated (Scheme 4).

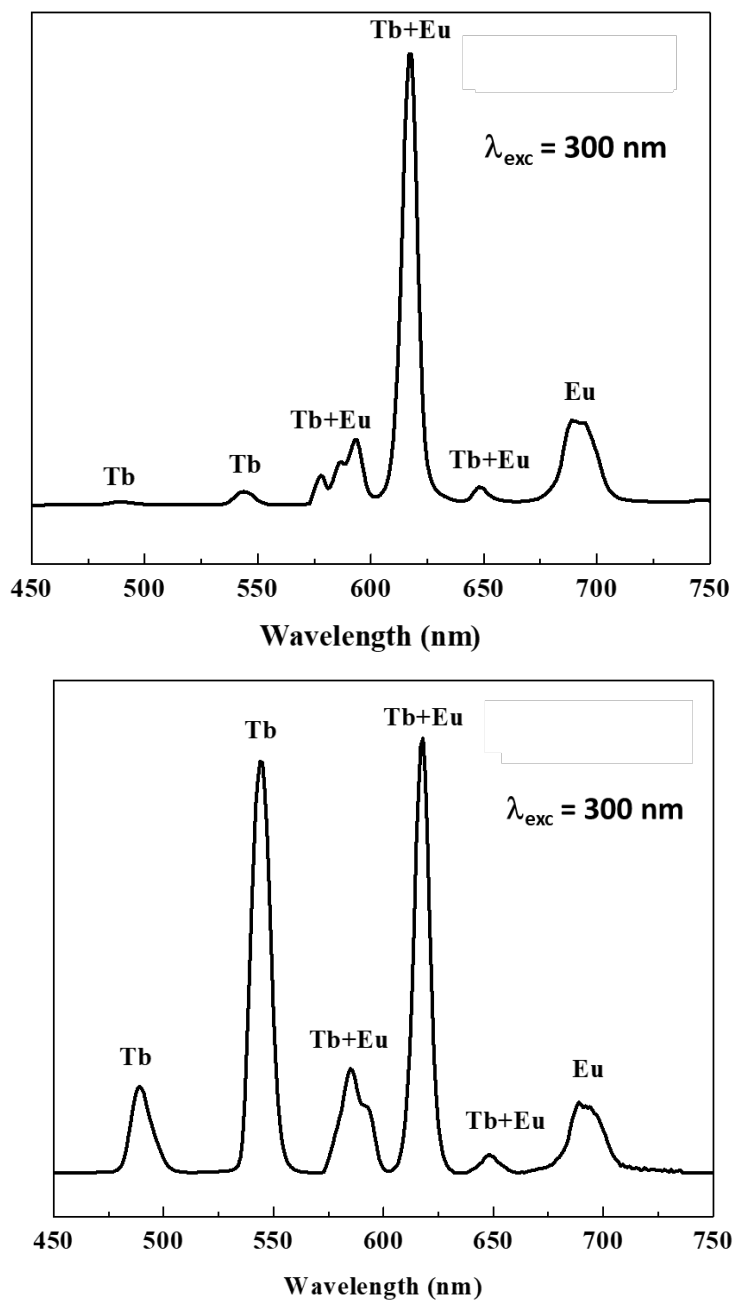
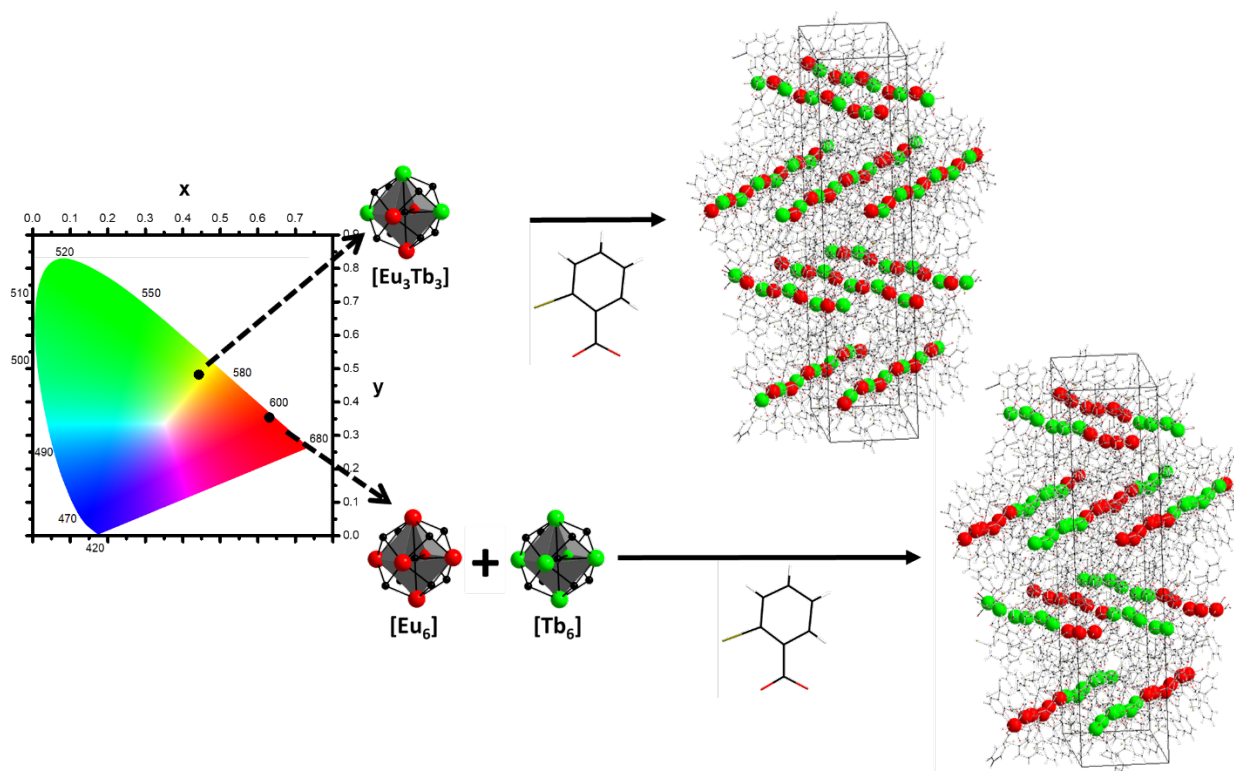


Figure 9. Room temperature solid-state emission spectra under UV irradiation ($\lambda_{exc} = 300$ nm) of $[\text{EuTb}(2\text{-bb})_6]_\infty$ (top) and $\{[\text{Tb}_2(2\text{-bb})_6]_{0.5}[\text{Eu}_2(2\text{-bb})_6]_{0.5}\}_\infty$ (down).

Both spectra are very different: (i) $[\text{EuTb}(2\text{-bb})_6]_\infty$ shows very weak Tb^{3+} luminescence intensity and the ratio (F) between the intensity of the Tb^{3+} dominant transition centered at 545 nm ($^5\text{D}_4 \rightarrow ^7\text{F}_5$) and that of the Eu^{3+} centered at 617 nm ($^5\text{D}_0 \rightarrow ^7\text{F}_2$) is only $F = 0.03$. Accordingly, this compound exhibits red emission ($x = 0.631$, $y = 0.354$). (ii) On the contrary,

$\{[\text{Tb}_2(2\text{-bb})_6]_{0.5}[\text{Eu}_2(2\text{-bb})_6]_{0.5}\}_\infty$ shows almost identical Tb^{3+} and Eu^{3+} emission intensities ($F = 0.94$) and therefore exhibits yellow emission ($x = 0.443$, $y = 0.482$) (Scheme 4).

These measurements are in perfect agreement with our suggested mechanism. Indeed, they strongly suggest that Tb^{3+} ions and Eu^{3+} ions are "segregated" in $\{[\text{Tb}_2(2\text{-bb})_6]_{0.5}[\text{Eu}_2(2\text{-bb})_6]_{0.5}\}_\infty$ while they are randomly distributed in $[\text{EuTb}(2\text{-bb})_6]_\infty$. According to us, it demonstrates that it is possible to design hetero-lanthanide coordination polymers with segregated and alternating sequences that contain only one of the two lanthanide ions and others that contain only the second one. To the best of our knowledge, this is unprecedented.



Scheme 4. Colorimetric coordinates of the coordination polymers prepared from $[\text{Eu}_3\text{Tb}_3]$ hexa-nuclear precursor (top) and from a fifty-fifty mixture of $[\text{Eu}_6]$ and $[\text{Tb}_6]$ hexa-nuclear precursors (bottom).

Luminescence properties of $\{[\text{Y}_2(2\text{-bb})_6]_{0.8}[\text{Tb}_2(2\text{-bb})_6]_{0.1}[\text{Eu}_2(2\text{-bb})_6]_{0.1}\}_\infty$

It is also possible to move away these homo-metallic sequences from each other by inserting optically non-active ones. Actually a tri-lanthanide coordination polymer with

chemical formula $\{[Y_2(2\text{-bb})_6]_{0.8}[Tb_2(2\text{-bb})_6]_{0.1}[Eu_2(2\text{-bb})_6]_{0.1}\}_\infty$ has been prepared from the mixture of the corresponding three homo-lanthanide hexa-nuclear precursor. Its emission spectra has been recorded ($\lambda_{\text{exc}} = 300\text{nm}$) (Figure S6). In this emission spectrum, Tb^{3+} component is dominant ($F = 1.7$) and indeed, the compound emits in the green ($x = 0.405, y = 0.538$) (Figure 10). This enhancement of the relative intensity of the Tb^{3+} component is due to the introduction of Y^{3+} -based sequences that makes the Tb^{3+} -based sequences and the Eu^{3+} -based ones far from each other and therefore reduces intermetallic transfers between them.

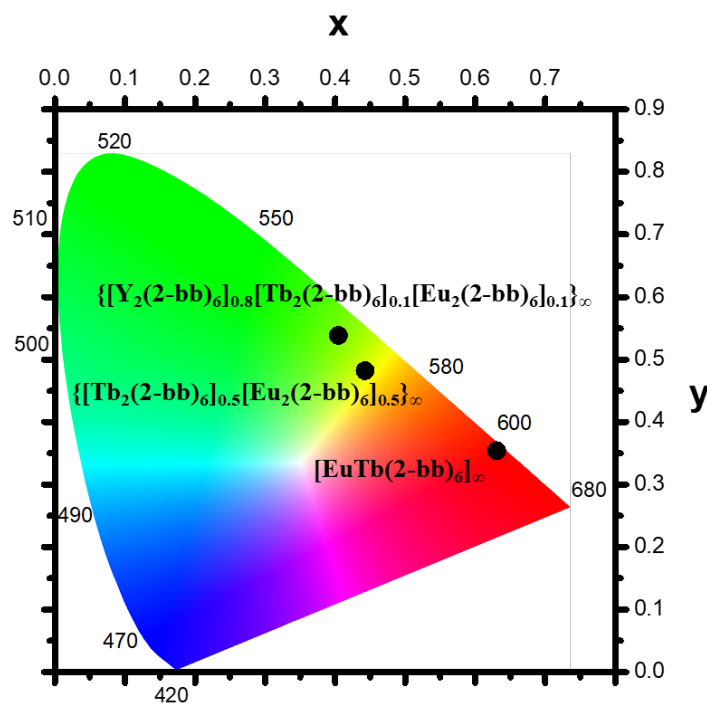


Figure 10. Colorimetric coordinates of $\{[Y_2(2\text{-bb})_6]_{0.8}[Tb_2(2\text{-bb})_6]_{0.1}[Eu_2(2\text{-bb})_6]_{0.1}\}_\infty$, $\{[Tb_2(2\text{-bb})_6]_{0.5}[Eu_2(2\text{-bb})_6]_{0.5}\}_\infty$ and $[EuTb(2\text{-bb})_6]_\infty$ under UV irradiation ($\lambda_{\text{exc}} = 300\text{ nm}$).

CONCLUSION AND OUTLOOK.

In this paper the crystal structure of a news series of iso-structural homo- and hetero-lanthanide coordination polymers with general chemical formula $[Ln_2(2\text{-bb})_6]_\infty$ is described. These compounds are prepared form hexa-nuclear molecular precursors.

Emission measurements suggest that the coordination of 2-bb⁻ ligand on a hexa-nuclear destroys this molecular precursor but somewhat preserve the relative arrangement of the six lanthanides. Indeed, optical signatures shows that the resulting coordination polymers present sequences of lanthanide ions that are reminiscent of the initial hexa-nuclear precursors. This leads to unprecedented coordination polymers in which the different lanthanide ions segregation can be controlled. This could be of great interest for materials tagging or fight against counterfeiting for which luminescent taggants difficult to replicate are needed. However, if technological applications are targeted, a scale up of the synthesis is mandatory. We are currently working along this line.

ACKNOWLEDGEMENTS.

The China Scholarship Council Ph.D. Program, a cooperation program with the French UT and INSA, is acknowledged for financial support. The CDIFX (diffraction center of Rennes) is acknowledged for the single crystals X-ray diffraction data collection. Miss Roxane Vadet is acknowledged for preparing some samples.

ASSOCIATED CONTENT.

Experimental X-ray powder pattern of $[\text{Dy}_2(2\text{-bb})_6]_\infty$ and simulated X-ray powder diagram of $[\text{Dy}_2(2\text{-bb})_6]_\infty$ from the crystal structure; IR spectrum of $[\text{Dy}_2(2\text{-bb})_6]_\infty$; Room temperature solid-state absorption spectrum of $[\text{Y}_2(2\text{-bb})_6]_\infty$; Solid-state emission spectrum of $[\text{Y}_2(2\text{-bb})_6]_\infty$ recorded at 77 K; Room temperature solid-state emission spectra of

$[\text{Y}_{2x}\text{Tb}_{2-2x}(\text{2-bb})_6]_\infty$ with $0.05 \leq x \leq 0.9$ ($\lambda_{\text{exc}} = 300$ nm). Room temperature solid-state emission spectrum of $\{[\text{Y}_2(\text{2-bb})_6]_{0.8}[\text{Tb}_2(\text{2-bb})_6]_{0.1}[\text{Eu}_2(\text{2-bb})_6]_{0.1}\}_\infty$

REFERENCES.

1. E. W. Berg; A. Alam, Studies on coordination polymers. Part I : Coordination polymers of 8,8'-dihydroxy-5,5'-biquinoyl. *Anal. Chim. Acta* 1962, **27**, 454-459.
2. Y. Cui; J. Zhang; H. He; G. Qian, Photonic functional metal–organic frameworks. *Chem. Soc. Rev.* 2018, **47**, 5740-5785.
3. Y. Cui; B. Li; H. He; W. Zhou; B. Chen; G. Qian, Metal-organic frameworks as platforms for functional materials. *Accounts Chem. Res.* 2016, **49**, 483-493.
4. Y. Cui; J. Zhang; B. Chen; G. Qian, Lanthanide Metal-Organic Frameworks for Luminescent Applications. *Handbook on the Physics and Chemistry of Rare Earths* 2016, **50**, 243-268.
5. B. Li; H.-M. Wen; Y. Cui; G. Qian; B. Chen, Multifunctional lanthanide coordination polymers. *Prog. Polym. Sci.* 2015, **48**, 40-84.
6. K. Bernot; C. Daugebonne; G. Calvez; Y. Suffren; O. Guillou, A Journey in Lanthanide Coordination Chemistry: From Evaporable Dimers to Magnetic Materials and Luminescent Devices. *Accounts Chem. Res.* 2021, **54**, 427-440.
7. O. Guillou; C. Daugebonne; G. Calvez; K. Bernot, A long journey in lanthanide chemistry : from fundamental crystallogenes studies to commercial anti-counterfeiting taggants. *Accounts Chem. Res.* 2016, **49**, 844-856.
8. J. C. G. Bünzli; S. V. Eliseeva, Intriguing aspect of lanthanide luminescence. *Chem. Sci.* 2013, **4**, 1039-1049.
9. S. V. Eliseeva; J. C. G. Bünzli, Rare earths : jewels for functional materials of the future. *New J. Chem.* 2011, **35**, 1165-1176.
10. R. Sessoli; K. Bernot, Lanthanides in extended molecular networks. In *Molecular magnetism*, Wiley-VCH Verlag GmbH & Co. KGaA: **2015**, p 89-124.
11. D. S. C. Brites; A. Millan; L. D. Carlos, Lanthanides in Luminescent Thermometry. In *Handbook on the Physics and Chemistry of Rare Earths*, Gschneidner, K. A.; Bünzli, J. C. G.; Pecharsky, V. K., Eds. Elsevier: **2016**; Vol. 49, p 339-427.
12. Y. Cui; R. Sog; J. Yu; M. Liu; Z. Wang; C. Wu; Y. Yang; Z. Wang; B. Chen; G. Qian, Dual emitting MOF-Dye composite for ratiometric temperature sensing. *Adv. Mater.* 2015, **27**, 1420-1425.
13. X. Rao; T. Song; J. Gao; Y. Cui; Y. Yang; C. Wu; B. Chen; G. Qian, A highly sensitive mixed lanthanide metal organic framework self calibrated luminescent thermometer. *J. Am. Chem. Soc.* 2013, **135**, 15559-15564.
14. V. Trannoy; A. N. C. Neto; D. S. C. Brites; L. D. Carlos; H. Serier-Brault, Engineering of mixed Eu³⁺/Tb³⁺ Metal-Organic Frameworks luminescent thermometers with tunable sensitivity. *Advanced Optical Materials* 2021, 2001938.
15. S. V. Eliseeva; J. C. G. Bünzli, Lanthanide luminescence for functional materials and bio-sciences. *Chem. Soc. Rev.* 2010, **39**, 189-227.
16. J.-C. G. Bünzli, Lanthanide luminescence for biomedical analyses and imaging. *Chem. Rev.* 2010, **111**, 2729-2755.
17. W. P. Lustig; S. Mukherjee; N. D. Rudd; A. V. Desai; J. Li; S. K. Ghosh, Metal–organic frameworks: functional luminescent and photonic materials for sensing applications. *Chem. Soc. Rev.* 2017, **46**, 3242-3285.
18. Z. Wang; Y. Yang; Y. Cui; Z. Wang; G. Qian, Color-tunable and white-light emitting lanthanide complexes based on (Ce_xEu_yTb_{1-x-y})₂(BDC)₃(H₂O)₄. *J. Alloys Compd.* 2012, **510**, L5-L8.
19. W. P. Lustig; J. Li, Luminescent metal organic frameworks and coordination polymers as alternative phosphors for energy efficient lighting devices. *Coord. Chem. Rev.* 2018, **373**, 116-147.
20. J. Andres; R. D. Hersch; J. E. Moser; A. S. Chauvin, A new counterfeiting feature relying on invisible luminescent full color images printed with lanthanide-based inks. *Adv. Func. Mater.* 2014, **24**, 5029-5036.

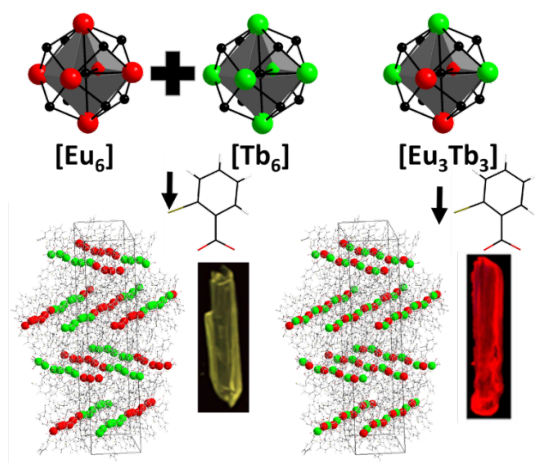
21. Y. Pointel; C. Daiguebonne; Y. Suffren; F. Le Natur; S. Freslon; G. Calvez; K. Bernot; D. Jacob; O. Guillou, Colloidal suspensions of highly luminescent lanthanide-based coordination polymer molecular alloys for ink-jet printing and tagging of technical liquids. *Inorg. Chem. Front.* 2021, 2125-2135.
22. D. A. Galico; A. A. Kitos; J. Ovens; F. A. Sigoli; M. Murugesu, Untapped potentials of lanthanide-based molecular clusteraggregates: optical barcoding and white-light emission with nanosized {Ln₂₀} compound. *Angew. Chem. Int. Ed.* 2021, **60**, 6130-6136.
23. K. A. White; D. A. Chengelis; K. A. Gogick; J. Stehman; N. L. Rosi; S. Petoud, Near infra-red luminescent lanthanide MOF barcodes. *J. Am. Chem. Soc.* 2009, **131**, 18069-18071.
24. J. C. G. Bünzli, On the design of highly luminescent lanthanide complexes. *Coord. Chem. Rev.* 2015, **293-294**, 19-47.
25. X. Fan; S. Freslon; C. Daiguebonne; L. Le Polles; G. Calvez; K. Bernot; O. Guillou, A family of lanthanide based coordination polymers with boronic acid as ligand. *Inorg. Chem.* 2015, **54**, 5534-5546.
26. S. V. Eliseeva; D. N. Pleshkov; K. A. Lyssenko; L. S. Lepnev; J. C. G. Bünzli; N. P. Kuzmina, Highly luminescent and triboluminescent coordination polymers assembled from Lanthanide beta-diketonate and aromatic bidentate O-donor ligands. *Inorg. Chem.* 2010, **49**, 9300-9311.
27. D. G. Karraker, Coordination of trivalent lanthanide ions. *J. Chem. Educ.* 1970, **47**, 424-430.
28. J. C. C. Santos; Y. Pramudya; M. Krstic; D.-H. Chen; B. L. Neumeier; C. Feldmann; W. Wenzel; E. Redel, Halogenated Terephthalic Acid "Antenna Effects" in Lanthanide-SURMOF Thin Films. *Applied Materials and Interfaces* 2020, **12**, 52166-52174.
29. A. Abdallah; S. Freslon; X. Fan; A. Rojo; C. Daiguebonne; Y. Suffren; K. Bernot; G. Calvez; T. Roisnel; O. Guillou, Lanthanide based coordination polymers with 1,4 carboxyphenylboronic ligand: multi emissive compounds for multi sensitive luminescent thermometric probes. *Inorg. Chem.* 2019, **58**, 462-475.
30. I. Badiane; S. Freslon; Y. Suffren; C. Daiguebonne; G. Calvez; K. Bernot; M. Camara; O. Guillou, High britness and easy color modulation in lanthanide-based coordination polymers with 5-methoxyisophthalate as ligand: Toward emission colors additive strategy. *Cryst. Growth Des.* 2017, **17**, 1224-1234.
31. G. E. Gomez; R. Marin; A. N. Carneiro Neto; A. M. P. Botas; J. Ovens; A. A. Kitos; M. C. Bernini; L. D. Carlos; G. J. A. A. Soler-Illia; M. Murugesu, Tunable Energy-Transfer Process in Heterometallic MOF Materials Based on 2,6-Naphthalenedicarboxylate: Solid-State Lighting and Near-Infrared Luminescence Thermometry. *Chem. Mater.* 2020, **32**, 7458-7468.
32. X. Feng; Y. Shang; H. Zhang; R. Li; W. Wang; D. Zhang; L. Wang; Z. Li, Enhanced luminescence and tunable magnetic properties of lanthanide coordination polymers based on fluorine substitution and phenanthroline ligand. *RSC Advances* 2019, **9**, 16328-16338.
33. V. Khudoleeva; L. Tceliykh; A. Kovalenko; A. Kalyakina; A. Goloveshkin; L. S. Lepnev; V. Utochnikova, Terbium-europium fluorides surface modified with benzoate and terephthalate anions for temperature sensing : Does sensitivity depends on the ligand ? *J. Lumin.* 2018, **201**, 500-508.
34. X. Liu; A. S.; S. H. C. Askes; I. Mutikainen; E. Bouwman, A novel coordination network of Tb(III) with 2-hydroxy-trimesic acid showing very intense photoluminescence. *Inorg. Chem. Comm.* 2015, **61**, 60-63.
35. Y. Luo; Y. Zheng; G. Calvez; S. Freslon; K. Bernot; C. Daiguebonne; T. Roisnel; O. Guillou, Synthesis, crystal structure and luminescent properties of new lanthanide-containing coordination polymers Involving 4,4'-oxy-bis-benzoate as Ligand. *Cryst. Eng. Comm.* 2013, **15**, 706-720.
36. B. V. Harbuzaru; A. Corma; F. Rey; P. Atienzar; J. L. Jorda; H. Garcia; D. Ananias; L. D. Carlos; J. Rocha, Metal-organic nanoporous structures with anisotropic photoluminescence and magnetic properties and their use as sensors. *Angew. Chem. Int. Ed.* 2008, **47**, 1080-1083.
37. R.-F. Li; R.-H. Li; X.-F. Liu; X.-H. Chang; X. Feng, Lanthanide complexes based on a conjugated pyridine carboxylate ligand: structures, luminescence and magnetic properties. *RSC Advances* 2020, **10**, 6192-6199.
38. X.-H. Wei; L.-Y. Yang; S.-Y. Liao; M. Zhang; J.-T. Tian; P.-Y. Du; W. Gu; X. Liu, A series of rare earth complexes with novel non-interpenetrating 3D networks: synthesis, structures, magnetic and optical properties. *Dalton Trans.* 2014, **43**, 5793-5800.

39. Y.-H. Luo; F.-X. Yue; X.-Y. Yu; X. Chen; H. Zhang, Coordination polymers of lanthanide complexes with benzene dicarboxylate ligands. *Cryst. Eng. Comm.* 2013, **15**, 6340-6348.
40. Y. Pointel; Y. Suffren; C. Daiguebonne; F. Le Natur; S. Freslon; G. Calvez; K. Bernot; O. Guillou, Rational design of dual IR and visible highly luminescent light lanthanides based coordination polymers. *Inorg. Chem.* 2020, **59**, 10673-10687.
41. Y. Pointel; F. Houard; Y. Suffren; C. Daiguebonne; F. Le Natur; S. Freslon; G. Calvez; K. Bernot; O. Guillou, High luminance of hetero lanthanide based molecular alloys by phase-induction strategy. *Inorg. Chem.* 2020, **59**, 11028-11040.
42. A. M. Badiane; S. Freslon; C. Daiguebonne; Y. Suffren; K. Bernot; G. Calvez; K. Costuas; M. Camara; O. Guillou, Lanthanide based coordination polymers with a 4,5-dichlorophthalate ligand exhibiting highly tunable luminescence : Toward luminescent bar codes. *Inorg. Chem.* 2018, **57**, 3399-3410.
43. X.-S. Wu; Y.-B. Zhang; X. Li; P. Z. Li, Two 1-D europium coordination polymers: synthesis, crystal structure and fluorescence. *J. Coord. Chem.* 2009, **62**, 797-807.
44. S. I. Weissman, Intramolecular energy transfer - The fluorescence of complexes of europium. *J. Chem Phys* 1942, **10**, 214-217.
45. G. Calvez; C. Daiguebonne; O. Guillou, Unprecedented lanthanide containing coordination polymers constructed from hexanuclear molecular building blocks: $\{[\text{Ln}_6\text{O}(\text{OH})_8](\text{NO}_3)_2(\text{bdc})(\text{Hbdc})_2, 2\text{NO}_3, \text{H}_2\text{bdc}\}_n$. *Inorg. Chem.* 2011, **50**, 2851-2858.
46. D. Alezi; A. M. P. Peedikakkal; L. Weselinski; V. Guillerme; Y. Belmabkhout; A. J. Cairns; Z. Chen; L. Wojtas; M. Eddaoudi, Quest for highly connected metal-organic framework platforms : rare earth polynuclear clusters versatility meets net topology needs. *J. Am. Chem. Soc.* 2015, **137**, 5421-5430.
47. L. Huang; L. Han; W. Feng; L. Zheng; Z. Zhang; Y. Xu; Q. Chen; D. Zhu; S. Niu, Two 3D Coordination Frameworks Based on Nanosized Huge Ln₂₆ (Ln = Dy and Gd) Spherical Clusters. *Cryst. Growth Des.* 2010, **10**, 2548-2552.
48. Z. Zheng, Assembling lanthanide hydroxo clusters. *Chemtracts - Inorganic Chemistry* 2003, **16**, 1-12.
49. R. Wang; H. Liu; M. D. Carducci; T. Jin; C. Zheng; Z. Zheng, Lanthanide coordination with alpha-amino acids under near physiological pH conditions : polymetallic complexes containing the cubane like $[\text{Ln}_4(\mu_3\text{-OH})_4]^{8+}$ cluster core. *Inorg. Chem.* 2001, **40**, 2743-2750.
50. Z. Zheng, ligand-controlled self-assembly of polynuclear lanthanide-oxo/hydroxo complexes : from synthetic serendipity to rational supramolecular design. *Chem. Comm.* 2001, 2521-2529.
51. Z. Zheng, Ligand-controlled self-assembly of polynuclear lanthanide-oxo/hydroxo complexes: from synthetic serendipity to rational supramolecular design. *Chem. Comm.* 2001, 10.1039/b107971a, 2521-2529.
52. G. Calvez; F. Le Natur; C. Daiguebonne; K. Bernot; Y. Suffren; O. Guillou, Lanthanide-based hexanuclear complexes and their use as molecular precursors. *Coord. Chem. Rev.* 2017, **340**, 134-153.
53. G. Giester; Z. Zak; P. Unfried, Syntheses and crystal structures of rare earth basic nitrates hydrates. *J. Alloys Compd.* 2009, **481**, 116-128.
54. G. Giester; Z. Zak; P. Unfried, Syntheses and crystal structures of rare earth basic nitrates hydrates: Part III. $[\text{Ln}_6(\mu_6\text{-O})(\mu_3\text{-OH})_8(\text{H}_2\text{O})_{12}(\text{NO}_3)_6](\text{NO}_3)_2 \cdot x\text{H}_2\text{O}$, Ln=Y, Sm, Eu, Gd, Tb, Dy, Ho, Er, Tm, Yb, Lu; x=0;3, 4, 5, 6. *J. Alloys Compd.* 2009, **481**, 116-128.
55. G. Giester; P. Unfried; Z. Zak, Syntheses and crystal structures of some new rare earth basic nitrates II : $[\text{Ln}_6\text{O}(\text{OH})_8(\text{H}_2\text{O})_{12}(\text{NO}_3)_6](\text{NO}_3)_2 \cdot x\text{H}_2\text{O}$, Ln=Sm, Dy, Er ; x(Sm)=6, x(Dy)=5, x(Er)=4. *J. Alloys Compd.* 1997, **257**, 175-181.
56. Z. Zak; P. Unfried; G. Giester, The structures of some rare earth basic nitrates $[\text{Ln}_6(\mu_6\text{-O})(\mu_3\text{-OH})_8(\text{H}_2\text{O})_{12}(\text{NO}_3)_6](\text{NO}_3)_2 \cdot x\text{H}_2\text{O}$, Ln=Y, Gd, Yb ; x(Y, Yb)=4, x(Gd)=5. A novel rare earth metal cluster of the M_6X_8 type with interstitial O atom. *J. Alloys Compd.* 1994, **205**, 235-242.
57. G. Calvez; C. Daiguebonne; O. Guillou; T. Pott; P. Méléard; F. Le Dret, Lanthanide-based hexanuclear complexes usable as molecular precursor for new hybrid materials : state of the art. *C. R. Chimie* 2010, **13**, 715-730.

58. H. Yao; G. Calvez; C. Daiguebonne; K. Bernot; Y. Suffren; M. Puget; C. Lescop; O. Guillou, Hexalanthanide complexes as molecular precursors: synthesis, crystal structure and luminescent and magnetic properties. *Inorg. Chem.* 2017, **56**, 14632-14642.
59. H. Yao; G. Calvez; C. Daiguebonne; K. Bernot; Y. Suffren; O. Guillou, Hetero-hexalanthanide complexes: A new synthetic strategy for molecular thermometric probes. *Inorg. Chem.* 2019, **58**, 16180-16193.
60. F. Le Natur; G. Calvez; J. P. Guégan; L. Le Polles; X. Trivelli; K. Bernot; C. Daiguebonne; C. Neaime; K. Costuas; F. Grasset; O. Guillou, Characterization and luminescence properties of lanthanide based polynuclear complexes nanoaggregates. *Inorg. Chem.* 2015, **54**, 6043-6054.
61. O. Guillou; C. Daiguebonne; G. Calvez; F. Le Dret; P. E. Car, Structuring effect of $[\text{Ln}_6\text{O}(\text{OH})_8(\text{NO}_3)_6(\text{H}_2\text{O})_{12}]^{2+}$ entities. *J. Alloys Compd.* 2008, **451**, 329-333.
62. G. Calvez; K. Bernot; O. Guillou; C. Daiguebonne; A. Caneschi; N. Mahé, Sterically-induced synthesis of 3d-4f one-dimensional compounds: a new route towards 3d-4f Single Chain Magnets. *Inorg. Chim. Acta* 2008, **361**, 3997-4003.
63. J. F. Desreux, In *Lanthanide Probes in Life, Chemical and Earth Sciences*, Choppin, G. R.; Bünzli, J. C. G., Eds. Elsevier: Amsterdam, **1989**; Vol. Elsevier, p 43.
64. G. Calvez; C. Daiguebonne; O. Guillou; F. Le Dret, A New Series of Anhydrous Lanthanide-Based Octahedral Hexanuclear Complexes. *Eur. J. Inorg. Chem.* 2009, **21**, 3172-3178.
65. F. Le Natur; G. Calvez; C. Daiguebonne; O. Guillou; K. Bernot; J. Ledoux; L. Le Polles; C. Roiland, Coordination polymers based on hexanuclear rare earth complexes : Toward independant luminescence brightness and color emission. *Inorg. Chem.* 2013, **52**, 6720-6730.
66. W. Kraus; G. Nolze, POWDER CELL - A program for the representation and manipulation of crystal structures and calculation of the resulting X-ray powder patterns. *J. Appl. Crystallogr.* 1996, **29**, 301-303.
67. T. Roisnel; J. Rodriguez-Carjaval, A Window Tool for Powder Diffraction Patterns Analysis. *J. Mater. Sci. Forum* 2001, **378**, 118-123.
68. T. Roisnel; J. Rodriguez-Carjaval, WinPLOT: a windows tool for powder diffraction pattern analysis. *Materials Science Forum, Proceedings of the Seventh European Powder Diffraction Conference (EPDIC 7)* 2000, 118-123.
69. A. Altomare; M. C. Burla; M. Camalli; G. Cascarano; C. Giacovazzo; A. Guagliardi; A. G. G. Moliterni; G. Polidori; R. Spagna, SIR97: a new tool for crystal structure determination and refinement *J. Appl. Crystallogr.* 1999, **32**, 115-119.
70. G. M. Sheldrick, A short history of SHELX. *Acta Crystallogr. A* 2008, **64**, 112-122.
71. G. M. Sheldrick; T. R. Schneider, SHELXL : High-Resolution Refinement. *Macromol. Crystallogr. B* 1997, 319-343.
72. L. J. Farrugia, WinGX suite for smallmolecule single-crystal crystallography. *J. Appl. Crystallogr.* 1999, **32**, 837-838.
73. L. J. Farrugia, WinGX and ORTEP for Windows: an update. *J. Appl. Crystallogr.* 2012, **45**, 849-854.
74. R. H. Blessing, An empirical correction for absorption anisotropy. *Acta Crystallogr.* 1995, **A51**, 33-38.
75. A. S. Chauvin; F. Gummy; D. Imbert; J. C. G. Bünzli, Europium and terbium tris(dipicolinate) as secondary standards for quantum yield determination. *Spectrosc Lett* 2004, **37**, 512-532.
76. G. Wyszecki, Colorimetry. In *Handbook of Optics*, Driscoll, W. G.; Vaughan, W., Eds. Mac Graw-Hill Book Company: New-York, **1978**, p 1-15.
77. CIE, *International Commission on Illumination - Technical report*. CIE: **1995**; Vol. 13-3, p 16.
78. D. Casanova; M. Llunell; P. Alemany; S. Alvarez, The rich stereochemistry of eight-vertex polyhedra: A continuous shape measures study. *Chem. - Eur. J.* 2005, **11**, 1479-1494.
79. S. Alvarez, Polyhedra in (inorganic) chemistry. *Dalton Trans.* 2005, 2209-2233.
80. D. L. Dexter, A theory of sensitized luminescence in solids. *J. Chem. Phys.* 1953, **21**, 836-850.
81. T. Förster, *Comparative effects of radiation*. John Wiley & Sons: New-York, **1960**.

82. C. Piguet; J. C. G. Bünzli; G. Bernardinelli; G. Hopfgartner; A. F. Williams, Self-assembly and photophysical properties of lanthanide dinuclear triple-helical complexes. *J. Am. Chem. Soc.* 1993, **115**, 8197-8206.
83. J. C. G. Bünzli; S. V. Eliseeva, Basics of lanthanide photophysics. In *Lanthanide Luminescence*, Hänninen, P.; Härmä, H., Eds. Springer Berlin Heidelberg: **2010**; Vol. 7, p 1-45.
84. F. J. Steemers; W. Verboom; D. N. Reinhoudt; E. B. Van der Tol; J. W. Verhoeven, New sensitizer-modified calix[4]arenes enabling Near-UV Excitation of complexed luminescent lanthanide ions. *J. Am. Chem. Soc.* 1995, **117**, 9408-9414.
85. M. Latva; H. Takalo; V.-M. Mikkala; C. Matachescu; J. C. Rodriguez-Ubis; J. Kankare, Correlation between the lowest triplet state energy level of the ligand and lanthanide luminescence quantum yields. *J. Lumin.* 1997, **75**, 149-169.
86. W. T. Carnall; P. R. Fields; K. Rajnak, Electronic energy levels of the trivalent lanthanide ions. IV. Eu^{3+} . *J. Chem. Phys.* 1968, **49**, 4450-4455.
87. V. Haquin; M. Etienne; C. Daiguebonne; S. Freslon; G. Calvez; K. Bernot; L. Le Polles; S. E. Ashbrook; M. R. Mitchell; J. C. G. Bünzli; O. Guillou, Color and brightness tuning in hetero-nuclear lanthanide teraphthalate coordination polymers. *Eur. J. Inorg. Chem.* 2013, 3464-3476.
88. R. Maouche; S. Belaid; B. Benmerad; S. Bouacida; C. Daiguebonne; Y. Suffren; S. freslon; K. Bernot; O. Guillou, Highly luminescent Europium-based heteroleptic coordination polymers with phenantroline and glutarate ligands. *Inorg. Chem.* 2021, **60**, 3707-3718.
89. F. Auzel, History of upconversion discovery and its evolution. *J. Lumin.* 2020, **223**, 116900.
90. F. Auzel, Upconversion and Anti-Stokes Processes with f and d Ions in Solids. *Chem. Rev.* 2004, **104**, 139-173.
91. L. Aboshyan-Sorgho; M. Cantuel; S. Petoud; A. Hauser; C. Piguet, Optical sensitization and upconversion in discrete polynuclear chromium–lanthanide complexes. *Coord. Chem. Rev.* 2012, **256**, 1644-1663.
92. M. Inokuti; F. Hirayama, Influence of Energy Transfer by the Exchange Mechanism on Donor Luminescence. *J. Chem. Phys.* 1965, **43**, 1978-1989.
93. J. C. G. Bünzli, Solvation and anion interaction in organic solvents. In *Handbook on the Physics and Chemistry of Rare Earths*, Gschneider, K. A.; Eyring, L., Eds. Elsevier: **1995**; Vol. 21, p 305-366.

TABLE OF CONTENT



The use of hexa-nuclear complexes as molecular precursors allows the design of hetero-lanthanide coordination polymers in which the lanthanides ions are organized in sequences or randomly distributed.